Estimation of the circumsolar ratio in a turbid atmosphere

Yehia Eissa, Philippe Blanc, Armel Oumbe, Hosni Ghedira, Lucien Wald

Available online at www.sciencedirect.com

ScienceDirect

Energy Procedia 57 (2014) 1169 – 1178

Energy Procedia

2013 ISES Solar World Congress

Estimation of the circumsolar ratio in a turbid atmosphere

Yehia Eissa[a,b,*], Philippe Blanc[a], Armel Oumbe[c], Hosni Ghedira[b], Lucien Wald[a]

[a]*MINES ParisTech, Centre Observation, Impacts, Energy, CS 10207 – 06904 Sophia Antipolis cedex, France*
[b]*Masdar Institute, Research Center for Renewable Energy Mapping and Assessment, Abu Dhabi, 54224, UAE*
[c]*Total New Energies, R&D – Concentrated Solar Technologies, 92069 Paris La Défense, France*

Abstract

Routine measurements of the direct normal irradiance (*DNI*) are not sufficient for optimal design of concentrating solar technologies. Due to a generally larger aperture angle of pyrheliometers or equivalent pyranometric systems when compared to that of concentrating collectors, the measured irradiance is overestimated as it includes the irradiance from the solar disc and a larger circumsolar region. The angular distribution of the direct and circumsolar radiances, *i.e.* the sunshape, can have a significant effect on the performance of concentrating collectors. Therefore, optimal design of concentrating solar technologies requires accurate measurements or estimations of the *DNI* and the sunshape. Published models are available for reproducing the representative sunshape for a given circumsolar ratio (*CSR*), *i.e.* the ratio between the circumsolar irradiance and the sum of the circumsolar and solar disc irradiances. The objective of this study is to estimate the *CSR* over a cloudless turbid atmosphere using a published sky radiance model and a Radiative Transfer Model (RTM). Using 10 months of solar irradiance and aerosol optical depth measurements, results show that there is an underestimation in the *CSR* computed by means of the sky radiance model when compared to that computed by the RTM. Also, a high correlation coefficient of 0.87 was found between the *CSR* estimated from both models, implying that modifications to the sky radiance model are possible to accurately estimate the *CSR*.

Selection and/or peer-review under responsibility of ISES.

Keywords: circumsolar radiation; circumsolar ratio; sky radiance; sunshape

* Corresponding author. Tel.: +33 (0)4 93 95 74 65; fax: +33 (0)4 93 67 89 08.
E-mail addresses: yehia.eissa@mines-paristech.fr (Y. Eissa), philippe.blanc@mines-paristech.fr (Ph. Blanc), armel.oumbe-ndeffotsing@total.com (A. Oumbe), hghedira@masdar.ac.ae (H. Ghedira), lucien.wald@mines-paristech.fr (L. Wald).

Selection and/or peer-review under responsibility of ISES.
doi:10.1016/j.egypro.2014.10.104

Nomenclature

a, b, c, d, e, f	adjustable coefficients defined by lookup tables in the all-weather model (unitless)
AOD	aerosol optical depth with subscript denoting the wavelength in nm (unitless)
AWM	subscript to indicate the variable was computed using the all-weather model
BHI_S	beam horizontal irradiance, within the extent of the solar disc only (W m^{-2})
$CSNI$	circumsolar normal irradiance (W m^{-2})
CSR	circumsolar ratio (unitless)
DHI	diffuse horizontal irradiance (W m^{-2})
DNI_S	direct normal irradiance, within the extent of the solar disc only (W m^{-2})
DNI	direct normal irradiance, including the $CSNI$ (W m^{-2})
GHI	global horizontal irradiance (W m^{-2})
I_0	solar constant corrected with respect to the Earth-Sun distance (W m^{-2})
lRt	subscript to indicate the variable was computed using the libRadtran Radiative Transfer Model
lv	relative luminance of a considered sky element (unitless)
m	air mass (unitless)
MBE	mean bias error (same units as the variable)
r	correlation coefficient (unitless)
R	radiance of the considered sky element (W m^{-2} sr^{-1})
rMBE	relative MBE (%) with respect to the mean reference value
RMSE	root mean square error (same units as the variable)
rRMSE	relative RMSE (%) with respect to the mean reference value
rSD	relative standard deviation of the difference (%) with respect to the mean reference value
SD	standard deviation of the difference (same units as the variable)
α	Ångström's coefficient (unitless)
Δ	sky brightness (unitless)
ε	sky clearness index (unitless)
ζ	zenith angle of the considered sky element (rad)
θ_Z	solar zenith angle (rad)
θ	angular distance from the center of the solar disc (rad)
φ	element azimuth angle (rad)

1. Introduction

Design of concentrating solar technologies (CSTs), including concentrating solar thermal electric power plants and concentrating photovoltaics, requires accurate knowledge of the solar radiant flux incident on the receiver. However, direct normal irradiance (*DNI*) measurements with pyrheliometers or equivalent pyranometric systems alone are not sufficient for the design of CSTs [1–3]. The angular distribution of the solar intensity in the vicinity of the direction of the Sun, *i.e.* the sunshape, has a significant effect on the performance of CSTs. Due to changes in the sunshape only, variations of up to 20% in the optical performance have been reported [1]. Small angle forward scattering, Mie scattering and particular cloud coverage, *e.g.* ice crystals such as cirrus, transfers part of the energy from the exact direction of the Sun to the circumsolar region causing different sunshapes. Recent pyrheliometers have an aperture half-angle typically ranging from 2.5° to 5° as recommended by the WMO CIMO guide [4], meaning that the measured *DNI* includes both the radiation received from the solar disc and that from a larger circumsolar region than typical acceptance angles of concentrating collectors [2,5].

The circumsolar ratio (*CSR*) is defined as the ratio between the radiant flux within a circumsolar region defined by its aperture half-angle and that within both the circumsolar region and solar disc [1,2]. Buie *et al.* [1] and Neumann *et al.* [6] have proposed representative sunshapes for given *CSR* values. In addition to *DNI* measurements, *CSR* measurements or estimations are also important for a proper design of CSTs.

The objective of this study is to present *CSR* values over a cloudless turbid atmosphere using a sky radiance model and a Radiative Transfer Model (RTM). The model of Perez *et al.* [7], named the all-weather model (AWM), and the libRadtran RTM [8] were employed to compute the *CSR*. The dataset utilized in this study comprised of 10 months of solar irradiance (global, diffuse and direct normal) and aerosol optical depth (*AOD*) measurements collected at Masdar City located in Abu Dhabi, United Arab Emirates (UAE). A comparison of the *CSR* estimated from both models was also conducted.

2. Methodology

2.1. Circumsolar ratio

The *CSR* is defined as the ratio of the circumsolar normal irradiance (*CSNI*) to the sum of the *CSNI* and the direct normal irradiance within the extent of the solar disc only (DNI_S) [1,2]. The outer limit of the circumsolar region is usually defined according to the aperture half-angle of the *DNI* measuring instrument. For example, Buie *et al.* [1] set it at 2.5°, which was the limit of the active cavity radiometer used to measure the *DNI* in the dataset they utilized. The limit of 2.5° is common, as it matches the aperture half-angle of primary standard pyrheliometers [4], this limit was employed in this study. The inner limit of the circumsolar region was set at 0°, *i.e.* the center of the solar disc. In this manner the *CSNI* accounts for the forward scattered solar beams within both the solar disc and the region between the edge of the solar disc and the aperture half-angle. DNI_S accounts for only the direct normal irradiance which has not undergone any scattering.

2.2. All-weather model

Perez *et al.* presented the AWM model that describes the sky luminance distribution using routine solar irradiance measurements for all sky conditions [7]. This model has been successfully applied in literature to estimate the sky radiances [9]. The radiance of a sky element defined by its zenith angle (ζ) and its angular distance (θ) with respect to the position of the Sun was computed by Eqs. (1) – (4).

$$R(\zeta, \theta) = \frac{lv(\zeta, \theta)}{\int_{\varphi=0}^{2\pi} \int_{\zeta=0}^{\pi/2} lv(\zeta, \theta) \cos\zeta \sin\zeta \mathrm{d}\zeta \mathrm{d}\varphi} DHI \quad (1)$$

$$lv = [1 + a \exp(b / \cos\zeta)] \times [1 + c \exp(d\theta) + e \cos^2 \theta] \quad (2)$$

$$\varepsilon = \frac{\frac{DHI + DNI}{DHI} + 1.041\theta_Z^3}{1 + 1.041\theta_Z^3} \quad (3)$$

$$\Delta = \frac{m DHI}{I_0} \quad (4)$$

where R is the radiance of the sky element angle defined by ζ and θ, φ is the azimuth angle of the sky element, lv is the relative luminance of the considered sky element, ε is the sky clearness index, θ_Z is the solar zenith angle in radians, Δ is the sky brightness and a, b, c, d and e are adjustable coefficients defined by lookup tables of ε and Δ [7]. I_0 is the solar constant – *i.e.* top of atmosphere normal irradiance – corrected with respect to Earth-Sun distance, the diffuse horizontal irradiance (*DHI*) and *DNI* are ground measured values and m is the air mass [10].

The erratum of the AWM is not significant over the environment of the dataset used, as only 21 of the 8667 observations match the condition in the erratum [11].

In this study, the AWM has been employed to estimate the sky radiances for the whole sky vault for a dataset covering 10 months over the desert environment of the UAE. The radiances from the circumsolar region, for an aperture half-angle of 2.5° – *i.e.* 43.6 mrad – from the center of the solar disc, were used to compute the AWM *CSNI* ($CSNI_{AWM}$) by Eq. (5). The estimated $CSNI_{AWM}$ was then divided by the ground measured *DNI*, to calculate the *CSR*, in this case labeled CSR_{AWM} (*cf.* Eq. (6)).

$$CSNI_{AWM} = \int_{\varphi=0}^{2\pi} \int_{\theta=0}^{43.6\ \mathrm{mrad}} R(\theta, \varphi) \sin(\theta) d\theta d\varphi \quad (5)$$

$$CSR_{AWM} = \frac{CSNI_{AWM}}{DNI} \quad (6)$$

2.3. Solar radiances and irradiances from the libRadtran Radiative Transfer Model

The libRadtran RTM is a software for radiative transfer calculations in the Earth's atmosphere [8]. For defined atmospheric and surface conditions, libRadtran has been successfully applied in computing the surface broadband radiances and irradiances in the solar spectrum [12,13].

The main parameters used in this study to define the surface and atmospheric characteristics were: the standard atmospheric profile chosen as mid-latitude summer, the *AOD* at 550 nm (AOD_{550}), the aerosol type chosen as desert, the total water column, the altitude of the site above sea level, the surface albedo,

the day of the year, the solar zenith angle and the solar azimuth angle. From the AERONET data, AOD_{550} is computed and the total water column is extracted, as explained later in Sect. 3.

LibRadtran was employed to compute the beam horizontal irradiance ($BHI_{S\text{-}lRt}$), *i.e.* beams within the solar disc only, which is assumed to be a point source by libRadtran. The direct normal irradiance incident from the solar disc only ($DNI_{S\text{-}lRt}$) was then computed by Eq. (7).

$$DNI_{S-lRt} = \frac{BHI_{S-lRt}}{\cos\theta_Z} \tag{7}$$

At a 0.1° resolution for θ and φ, the libRadtran RTM was also employed to compute the sky radiances in the circumsolar region, *i.e.* from the center of the solar disc to an aperture half-angle of 2.5°. Replacing subscript AWM with lRt in Eq. (5) the libRadtran *CSNI* ($CSNI_{lRt}$) was computed. The direct normal irradiance (DNI_{lRt}), including both the $CSNI_{lRt}$ and the $DNI_{S\text{-}lRt}$, was computed by Eq. (8). The *CSR* from libRadtran (CSR_{lRt}) was finally computed by Eq. (9).

$$DNI_{lRt} = CSNI_{lRt} + DNI_{S-lRt} \tag{8}$$

$$CSR_{lRt} = \frac{CSNI_{lRt}}{DNI_{lRt}} \tag{9}$$

3. Experimental setup

The applied dataset in this study consisted of ground measurements covering a period of 10 months, June 2012 to March 2013, collected at Masdar City, Abu Dhabi, UAE.

The solar irradiance measurements consisted of 10 minute averages of the global horizontal irradiance (*GHI*) and *DHI*, measured using a rotating shadowband irradiometer (RSI) located at 24.420 °N and 54.613 °E (7 m above sea level). The station was installed by CSP Services (http://www.cspservices.de) for the client Masdar Clean Energy.

The RSI comprised of a LI-COR LI-200 Pyranometer integrated with a rotating shadowband. This pyranometer was calibrated against an Eppley Precision Pyranometer under natural daylight conditions and has a spectral range from 400 nm to 1100 nm. During operation, the *GHI* is measured when the shadowband is stationary and the *DHI* is measured when the rotating shadowband blocks the whole solar disc. The *DNI* was computed from the *GHI* and *DHI* measurements.

All solar irradiance measurements were tested for two quality check tests from Roesch *et al.* for *GHI* measurements greater than 50 W m^{-2}, where the tests are not applicable for lower *GHI* values [14]. In the first test the conditions of Eq. (10) had to be fulfilled, while in the second test the conditions of Eq. (11) had to be true.

$$\begin{aligned} (DNI\cos\theta_Z + DHI)/GHI &= 1 \pm 0.08 \quad \text{for } \theta_Z \le 75° \\ (DNI\cos\theta_Z + DHI)/GHI &= 1 \pm 0.15 \quad \text{for } \theta_Z > 75° \end{aligned} \tag{10}$$

$$\begin{aligned} DHI/GHI &< 1.05 \quad \text{for } \theta_Z \le 75° \\ DHI/GHI &< 1.10 \quad \text{for } \theta_Z > 75° \end{aligned} \tag{11}$$

The first test does not seem fair, as the *DHI* and *GHI* were measured by the same instrument, and the *DNI* was computed from them. This test is more appropriate in case the three irradiances were measured by different instruments. Still, all measurements passed the quality check of both tests.

Also, available at Masdar city was the AERONET measurement station, comprising a CIMEL-318 Sun photometer, situated at 24.442 °N and 54.617 °E (4 m above sea level). The AERONET data which was used in this study included the aerosol optical depth at 675 nm (AOD_{675}), Ångström's coefficient (α) between 440 nm and 870 nm and the total water vapor column derived from the 935 nm channel [15].

The two ground stations are approximately 2.5 km apart. It is reasonable to assume that both stations exhibit almost the same atmospheric conditions as they are close and both situated in very similar environments. However, micro sandstorms could occur at one station and not the other during data acquisition. Also, in scattered cloud conditions, it can be cloudless at the instant of the AERONET acquisition, but cloudy over the RSI. The scattered cloud conditions could also occur even if both sensors were in the same location, as the solar irradiance measurements were 10 min averages whereas the AERONET measurements were instantaneous. These phenomena cause few ambiguities in the dataset.

Even though the aperture angle of the RSI is not clearly defined as the pyrheliometer, a comparison was conducted for one year of *DNI* computations from the RSI against *DNI* measurements from the pyrheliometer at a different station in the UAE. The pyrheliometer had an aperture half-angle of 2.5°. For a full year of *DNI* measurements higher than 200 W m^{-2}, a relative mean bias error (rMBE) of +0.31% and a relative root mean square error (rRMSE) of 2.9% were obtained. Since the bias is negligible between both instruments, it is assumed in this study that the RSI has pretty much the same aperture half-angle as the pyrheliometer. Wilbert *et al.* claim a 2.86° aperture half-angle for the RSI [16].

This specific dataset was selected based on data availability over the turbid atmosphere in the UAE. Masdar Institute is the only location in the UAE which has overlapping AERONET and solar irradiance measurements. The AERONET station in this location was installed in June 2012. Other solar radiation and AERONET stations in the UAE do not overlap in time or are over 15 km apart.

The downloaded AERONET data was level 1.5 data: meaning the dataset was already screened for cloudy observations [15]. For each AERONET observation, the two neighboring 10 min solar irradiance measurements were linearly interpolated to match the AERONET acquisition time.

The AOD_{550} is not directly measured by the Sun photometer of the AERONET station, instead it was computed using the measured AOD_{675} and α between 440 nm and 870 nm using Eq. (12) [17].

$$AOD_{550} = AOD_{675}\left(\frac{675}{550}\right)^{\alpha} \tag{12}$$

All in all, 8667 cloudless observations with both RSI and AERONET measurements remained in the dataset actually employed in this study. The dataset was evenly distributed throughout the sunlight hours. The months June to October and January to March had almost even distributions, where each month had between 9.8% and 13.5% of all measurements. The winter months of November and December each had ~ 5% of the dataset, which could be due to shorter sunlight hours and higher cloud coverage.

In the final dataset the *GHI* ranged from 91 W m^{-2} to 1011 W m^{-2}, the *DNI* from 5 W m^{-2} to 957 W m^{-2}, the *DHI* from 42 W m^{-2} to 579 W m^{-2}, the AOD_{550} from 0.04 to 1.9, the total water column from 0.33 cm to 5.17 cm and the θ_Z from 2.7° to 78.9°.

4. Results and discussion

4.1. CSR from the all-weather model

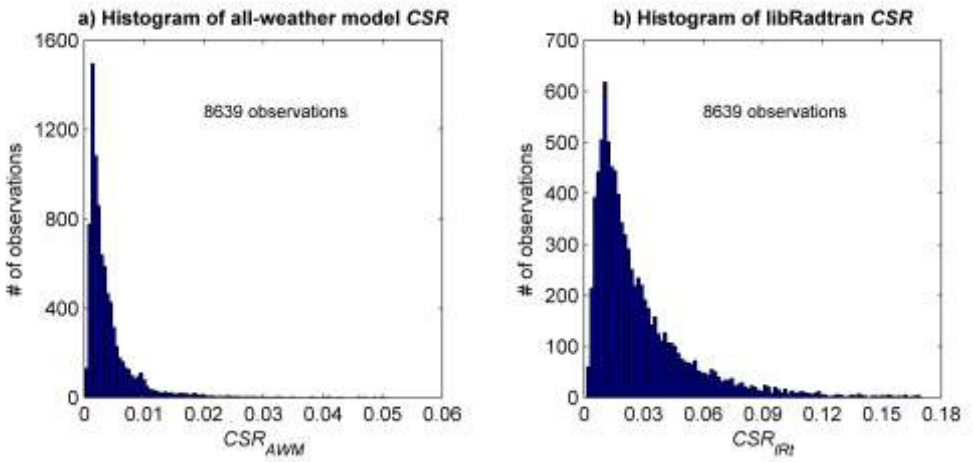

Fig. 1. (a) histogram (maximum value of P99.7) of the CSR_{AWM}; (b) histogram (maximum value of P99.7) of the CSR_{lRt}.

The AWM was used to compute the radiances across the whole hemispherical sky. Then the modeled radiances in the circumsolar region were used to derive CSR_{AWM}. Fig. 1a shows the distribution of CSR_{AWM} values for the employed dataset. CSR_{AWM} values seem to be very low: 92.5% of the observations exhibit a *CSR* lower than 0.01.

This number is very doubtful in the turbid atmosphere of the UAE. Indeed, using measurements collected over three sites in Europe, Neumann *et al.* report that 67% of their observations have a *CSR* between 0 and 0.04 [6]. Using sunshape profiles measured by the Sun and Aureole Measurement System (SAM) [5] during the days 5 to 7 September, 2012 in Masdar City, Kalapatapu *et al.* report no *CSR* values lower than ~ 0.08 [18], which is a value not present in the histogram of Fig. 1a.

The reasons causing those low *CSR* values from the AWM are that the model was validated only for sky areas with angular distances greater than 12° from the center of the Sun [19] and the coefficients in the AWM were fitted using luminance measurements in a totally different meteorological and aerological environment in Berkeley, California.

4.2. CSR from the libRadtran Radiative Transfer Model

Using the atmospheric and surface conditions along with geometric parameters, the libRadtran RTM was used to derive the sky radiances only in the circumsolar region up to a half-angle of 2.5°. The $CSNI_{lRt}$, $DNI_{S\text{-}lRt}$ and CSR_{lRt} were then computed as explained in Sect. 2.3.

As shown by the histogram of the CSR_{lRt} values presented in Fig. 1b, the CSR_{lRt} values were greater than those obtained using the AWM. Results show that 20% of the dataset had a *CSR* less than 0.01, while 78.5% had a *CSR* between 0 and 0.04. Those results are more comparable with the ones reports in Neumann *et al.* [6]. However, Neumann *et al.* collected measurements over three sites in Europe, which have different environmental characteristics than that of the UAE. It is assumed that the sites in Europe would exhibit more cirrus cloud conditions, while that in the UAE would exhibit more dusty conditions. Comparing between CSR_{lRt} and the *CSR* presented in Kalapatapu *et al.* during the days 5 to 7 September, 2012 in Masdar City, Kalapatapu *et al.* report no *CSR* values lower than ~ 0.08 while during the same times of those three days CSR_{lRt} values do not exceed ~ 0.04 [18]. Even though the CSR_{lRt} values are

underestimated with respect to those reported, three reference days are not enough to draw conclusions. Therefore, validating the CSR_{lRt} with SAM-derived *CSR* is an area requiring further work.

Validating the $DNI_{S\text{-}lRt}$ with respect to the ground measured *DNI*, an rRMSE of 8.7% and an rMBE of +2.4% were obtained. Validating DNI_{lRt} with respect to the ground measured *DNI*, an rRMSE of 9.2% and an rMBE of +4.4% were obtained. The scatter plots are presented in Fig. 2.

The outliers present in the Fig. 2 for *DNI* measurements ranging from 200 W m^{-2} to 600 W m^{-2} were mainly due to scattered cloud conditions as mentioned earlier in Sect. 3. The instant of AERONET data acquisition could be cloudless, but it can still be cloudy for part or most of the 10 min average of the solar irradiance measurement. This would cause an overestimation in DNI_{lRt}, which is the case as shown in Fig. 2. To confirm, the days of some of the outliers were visually observed using the high-resolution visible channel of the SEVIRI instrument on board Meteosat Second Generation satellite. The presence of scattered clouds over Masdar City was visually confirmed over all selected days.

In both cases there is a trend in the scatter plots of Fig. 2, where libRadtran overestimates almost all ground measured *DNI* values greater than 800 W m^{-2}. This may be caused by solar modeling error of libRadtran or instrument error, where the RSI has larger errors for larger measured values. This bias could also be due to the quality of some of the AERONET measurements. The data available over Masdar City was only screened for clouds (*i.e.* level 1.5), whereas the quality assured level 2.0 data was not available.

Still, libRadtran estimated values are reasonable, having low rRMSE and rMBE values. Also, the difference in bias between the DNI_{lRt} and $DNI_{S\text{-}lRt}$ is almost +2%, which is mainly due to the *CSNI*. The *CSNI* is not accounted for in $DNI_{S\text{-}lRt}$, but it is accounted for in DNI_{lRt}. Also, the standard deviation of the difference (SD) is 44.6 W m^{-2} for $DNI_{S\text{-}lRt}$ and 43.3 W m^{-2} for DNI_{lRt}. The slight improvement in the SD for DNI_{lRt} could again be due to accounting for the *CSNI* in DNI_{lRt}.

4.3. Comparison of all-weather model and libRadtran derived CSR

Comparing between the *CSNI* values of the AWM and libRadtran, an rRMSE of 91.4%, an rMBE of −86.1% and a correlation coefficient *r* of 0.91 were obtained, as presented in Fig. 3a.

Comparing between the *CSR* results of the AWM and libRadtran, it is clear that the AWM is highly underestimating the *CSR* when compared to those derived from libRadtran. The rMBE is −84.4%, showing that indeed the AWM underestimated the *CSR*.

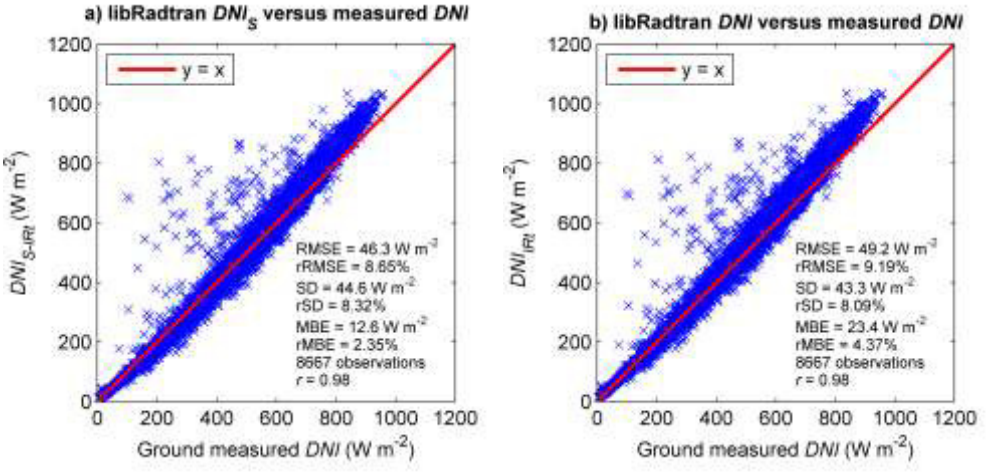

Fig. 2. (a) $DNI_{S\text{-}lRt}$ versus ground measured *DNI*; (b) DNI_{lRt} versus ground measured *DNI*.

On the bright side, there is a very high correlation coefficient *r* of 0.87 between the *CSR* of both models. The scatter plot between CSR_{AWM} and CSR_{lRt} is presented in Fig. 3b.

The correlation coefficient *r* between both models up to a CSR_{lRt} of 0.125, which makes up 98.7% of the dataset, is quite high with $r = 0.95$. In the CSR_{lRt} range between 0.125 and 0.16, there is still good correlation between both models, with $r = 0.84$, but it does not follow the same linear trend than the one for the *CSR* range from 0 to 0.125.

For CSR_{lRt} values greater than 0.16, the bias between both models is lower, with a relatively lower correlation, $r = 0.8$.

It is to be noted there are only 44 observations for CSR_{lRt} values greater than 0.16. Those 44 observations had *DNI* measurements ranging from 4.5 W m^{-2} to 34 W m^{-2}, and solar zenith angles ranging from 59° to 78.6°. Those low *DNI* values could be due to misclassification of cloudy observations as cloudless or from dusty conditions.

The quite high correlation between the *CSR* values in both models is very encouraging as it opens up room for improvements in sky radiance/luminance models in the circumsolar region. Sky radiance/luminance models with improvements in the circumsolar region would be useful as such models could provide quick and accurate computations of the sky radiance distribution for the whole sky vault using routine solar irradiance measurements, *i.e.* the *DNI*, *DHI* and *GHI*. As opposed to the drawbacks of the RTMs, which include a significantly longer processing time and the need for inputs which are not always available at high temporal resolutions like the aerosol optical depth, total water column, surface albedo and others depending on the configuration of inputs to the RTM.

5. Conclusion

CSR results over a cloudless turbid atmosphere show that the all-weather model largely underestimates the *CSR* values when compared to those derived by the libRadtran RTM or when compared to literature-based values. The high correlation between the *CSR* derived from both models opens interesting possibilities for improvement in sky radiance/luminance models in the circumsolar region, while preserving their good performance for hemispherical purposes, such as global tilt irradiance estimations.

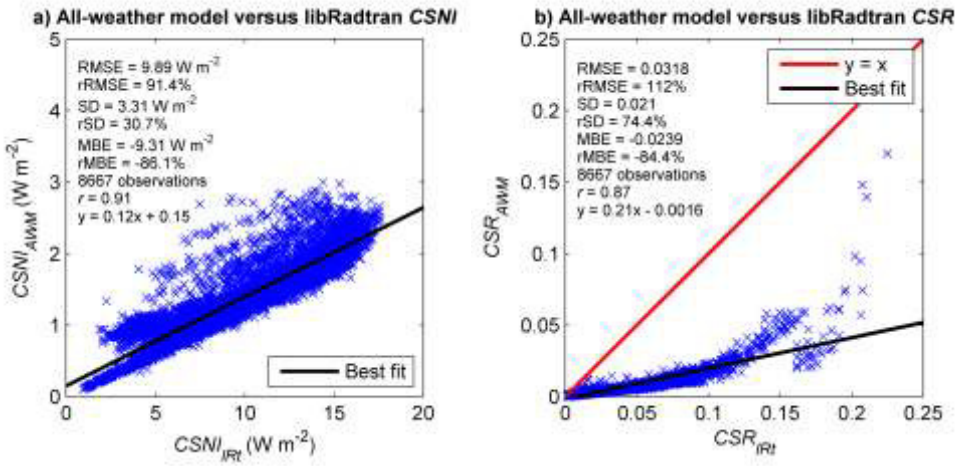

Fig. 3. (a) $CSNI_{AWM}$ versus $CSNI_{lRt}$; (b) CSR_{AWM} versus CSR_{lRt}.

The advantages of sky radiance/luminance models include faster processing times and inputs which are generally more available than those required by RTMs. Further areas to be exploited with regards to this work include comparing the *CSR* derived from RTMs and sky radiance models to *CSR* values derived through sunshape ground measurements. Fortunately, a Sun and Aureole Measurement System is available in the same location of this study. Also, comparisons between different sky radiance models would be essential to study how different models react in the circumsolar region. Finally, an improvement in the computed sky radiances of the circumsolar region would be beneficial for design purposes.

Acknowledgements

The research leading to these results has received funding from Total New Energies under the project PREDISOL. We thank Dr. Peter Armstrong and Dr. Matteo Chiesa for their efforts in installing and maintaining the Masdar Institute AERONET station.

References

[1] Buie D, Monger AG, Dey CJ. Sunshape distributions for terrestrial solar simulations. *Solar Energy* 2003;**74**:113–122.
[2] Rabl A, Bendt P. Effect of circumsolar radiation on performance of focusing collectors. *Journal of Solar Energy Engineering* 1982;**104**:237–250.
[3] Wilbert S, Pitz-Paal R, Jaus J. Circumsolar radiation and beam irradiance measurements for focusing collectors. In: Cost Wire ES1002 Workshop on Remote Sensing Measurements for Renewable Energy, 22-23 May 2012, Risoe, Denmark.
[4] WMO. Measurement of radiation. Guide to Meteorological Instruments and Methods of Observation, Geneva: World Meteorological Organization; 2008, 1.7:1–41.
[5] Wilbert S, Reinhardt B, Devore J, Röger M, Pitz-Paal R, Gueymard C. Measurement of solar radiance profiles with the sun and aureole measurement system (SAM). In: SolarPACES Conference, 20-23 September 2011, Granada, Spain.
[6] Neumann A, Witzke A, Jones SA, Schmitt G. Representative terrestrial solar brightness profiles. *Journal of Solar Energy Engineering* 2002;**124**:198–204.
[7] Perez R, Seals R, Michalsky J. All-weather model for sky luminance distribution - Preliminary configuration and validation. *Solar Energy* 1993;**50**:235–245.
[8] Mayer B, Kylling A. Technical note: The libRadtran software package for radiative transfer calculations - description and examples of use. *Atmospheric Chemistry and Physics* 2005;**5**:1855–1877.
[9] Gracia A, Torres JL, De Blas M, García A, Perez R. Comparison of four luminance and radiance angular distribution models for radiance estimation. *Solar Energy* 2011;**85**:2202–2216.
[10] Kasten F, Young AT. Revised optical air mass tables and approximation formula. *Applied Optics* 1989;**28**:4735–4738.
[11] Perez R, Seals R, Michalsky J. Erratum to all-weather model for sky luminance distribution - Preliminary configuration and validation. *Solar Energy* 1993;**51**:423.
[12] Lefèvre M, Oumbe A, Blanc P, Espinar B, Gschwind B, Qu Z, et al. McClear: a new model estimating downwelling solar radiation at ground level in clear-sky conditions. *Atmospheric Measurement Techniques Discussions* 2013;**6**:2403–2418.
[13] Oumbe A, Qu Z, Blanc P, Bru H, Lefèvre M, Wald L. Modeling circumsolar irradiance to adjust beam irradiances from radiative transfer models to measurements. In: 12th EMS Annual Meeting, 10-14 September 2012, Łódź, Poland.
[14] Roesch A, Wild M, Ohmura A, Dutton EG, Long CN, Zhang T. Assessment of BSRN radiation records for the computation of monthly means. *Atmospheric Measurement Techniques* 2011;**4**:339–354.
[15] http://aeronet.gsfc.nasa.gov/
[16] Wilbert S, Pitz-paal R, Müller S. Rotating shadowband irradiometers and circumsolar radiation. In: Cost Wire Workshop Payerne, 21 September 2012, Payerne, Switzerland.
[17] Banks JR, Brindley HE. Evaluation of MSG-SEVIRI mineral dust retrieval products over North Africa and the Middle East. *Remote Sensing of Environment* 2013;**128**:58–73.
[18] Kalapatapu R, Chiesa M, Armstrong P, Wilbert S. Measurement of DNI angular distribution with a sunshape profiling irradiometer. In: SolarPACES Conference, 11-14 September 2012, Marrakech, Morocco.
[19] Ineichen P, Molineaux B, Perez R. Sky luminance data validation: Comparison of seven models with four data banks. *Solar Energy* 1994;**52**:337–346.